

**Formation of ZnS Quantum Dots using Green Tea Extract: Applications into Protein  
binding, Bio-sensing, Anti-bacterial and Cell Cytotoxicity studies**

Mahabul Haque<sup>a</sup>, Ibemhanbi Konthoujam<sup>b</sup>, Sona Lyndem<sup>a</sup>, Sudipta Koley<sup>c</sup>, Kripamoy Aguan<sup>b</sup>,  
Atanu Singha Roy<sup>a,\*</sup>

<sup>a</sup>Department of Chemistry, National Institute of Technology Meghalaya, Shillong, 793003, India

<sup>b</sup>Department of Biotechnology & Bioinformatics, North-Eastern Hill University, Shillong  
793022, India

<sup>c</sup>Department of Physics, Amity University, Kolkata 700135, India

**\*Corresponding Author:** Atanu Singha Roy

Tel.: +91 364 2501294

Fax: +91 364 2501113

Email: singharoyatanu@gmail.com; asroy86@nitm.ac.in

## 1. Determination of Quantum yield

The quantum yield (QY) of synthesized ZnS-GT QDs was calculated using the previously reported comparison method<sup>1,2</sup>. Anthracene (in ethanol) was used as the standard reference for the determination of QY using the Eq. S1.

$$\Phi_{ZnS-GT} = \Phi_{Anthracene} \times \frac{\mu_{ZnS-GT}}{\mu_{Anthracene}} \times \left( \frac{n_{ZnS-GT}}{n_{Anthracene}} \right)^2 \quad (S1)$$

Where  $\phi_{Anthracene}$  and  $\phi_{ZnS-GT}$  denote the QY of ZnS-GT QDs and anthracene, respectively, the slopes of the graph of integrated fluorescence intensity vs absorbance represent the  $\mu_{ZnS-GT}$  and  $\mu_{Anthracene}$ , respectively. The refractive indices of the medium are  $n_{ZnS-GT}$  (1.33 for water as solvent) QDs and  $n_{Anthracene}$  (1.36 for ethanol as the solvent). Figure S1 depicted the integrated fluorescence intensity versus absorbance graph, and the QY of the ZnS-GT QDs was found to be  $\sim 12\%$  (11.99%) calculated using Eq S1.

## 2. Details stability studies of synthesized ZnS-GT QDs

The stability of synthesized ZnS-GT QDs was investigated in different pH (pH: 3, 5, 7, 9 of phosphate buffer) and in the presence of various metal ions (e.g.,  $Fe^{3+}$ ,  $Fe^{2+}$ ,  $K^+$ ,  $Mn^{2+}$ ,  $Ca^{2+}$ ,  $Cu^{2+}$ ,  $Co^{2+}$ ,  $Na^+$ , and  $Ni^{2+}$ ). The fluorescence intensity of ZnS-GT QDs in varied pH remained nearly constant after 30 days of storage, indicating that ZnS-GT QDs are stable at pH 3, 5, 7, and 9 (Figure S2), while the intensities of ZnS-GT were variable. The ZnS-GT QDs, on the other hand, were stable in the presence of metal ions (Figure S3, S4, and S5), with little increase in fluorescence intensity with storage time (up to 30 days), which is owing to the presences of metal ions affecting the band gap of ZnS-GT QDs<sup>3-5</sup>. Figure S5.b depicted the effect of temperature on the fluorescence intensity of synthesized ZnS-GT QDs; with the rise in temperature (from 20°C to 35°C) the fluorescence intensity was found to be decreased.



### 3. Synchronous fluorescence studies (SFS)

Llyod (1971)<sup>6</sup> suggested the use of synchronous fluorescence as a method for detecting changes that occur in the immediate area of a fluorophore as a result of ligand binding. According to Miller's theory<sup>7</sup>, the specific information regarding the microenvironment of the tryptophan (Trp) and tyrosine (Tyr) residues of the protein can be retrieved by maintaining the wavelength interval at a fixed value of 60 nm for Trp and 15 nm for Tyr respectively. This method is now extensively used to investigate the macro-environ changes around the protein fluorophore residues (Trp and Tyr) upon interaction with ligands, NPs, or QDs. Figure S7 represents the synchronous fluorescence profile of HSA upon dose-dependent titration of ligands (ligand: Que, Lut, and ZnS-GT QDs) at  $\Delta\lambda = 15$  nm (Tyr) and  $\Delta\lambda = 60$  nm (Trp). With increasing ligand concentrations, there is a constant decrease in HSA emission intensity, and a blue shift of 2 nm and 3 nm was observed for HSA-Que and HSA-Lut interactions (at  $\Delta\lambda = 60$  nm). This modest blue shift could be attributed to the relocation of the Trp residues towards a less polar environment; more specifically, the polarity around the Trp micro-environment lowers as a result of the association with Que and Lut. In contrast, a 6 nm red shift was found for the HSA-ZnS-GT QDs association (at  $\Delta\lambda = 60$  nm), which indicates the relocation of the Trp residues toward the more hydrophilic region of the protein environment. However, no change in the fluorescence peaks for  $\Delta\lambda = 15$  nm (Tyr) was observed, implying that the microenvironment around the Tyr moiety is not affected by association with the ligand. These findings corresponded well with the results of steady-state fluorescence studies, and it is clear that Trp residues take part in the binding interactions.

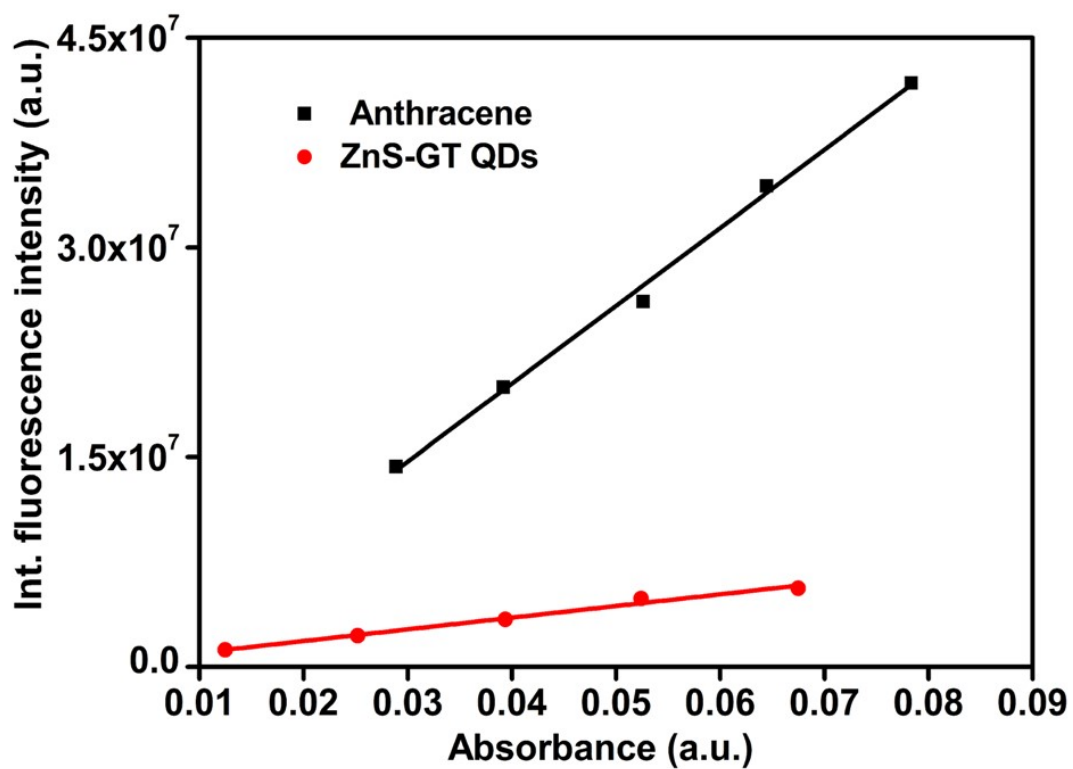


**Figure S1:** Calibration plot for the determination of quantum yield of ZnS-GT QDs using anthracene as a standard reference.

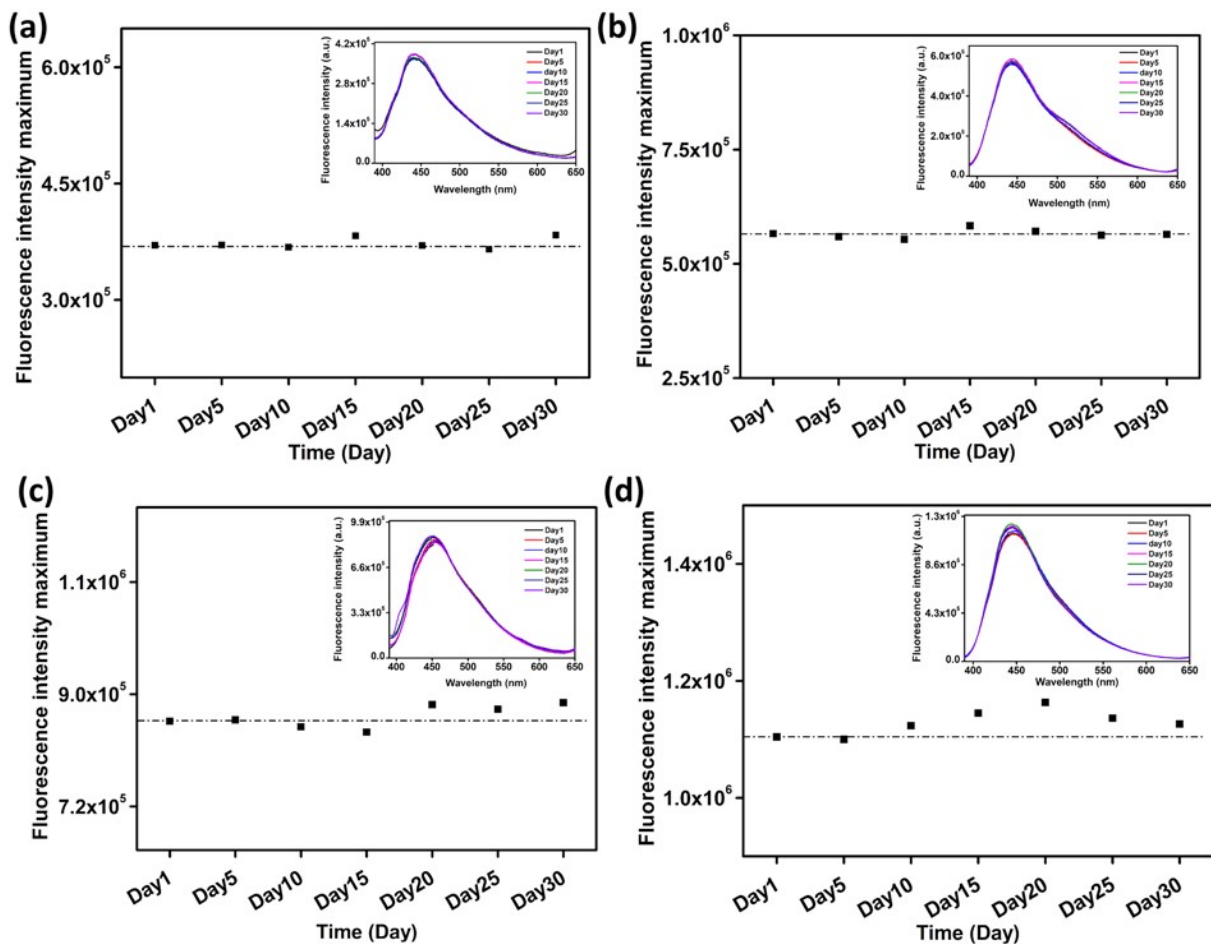


**Figure S2:** Variation of fluorescence intensity of synthesized ZnS-GT QDs as function of storage time at phosphate buffer (PB) of different pH. (a) pH 3.0, (b) pH 5.0, (c) pH 7.0 and (d) pH 9.0.

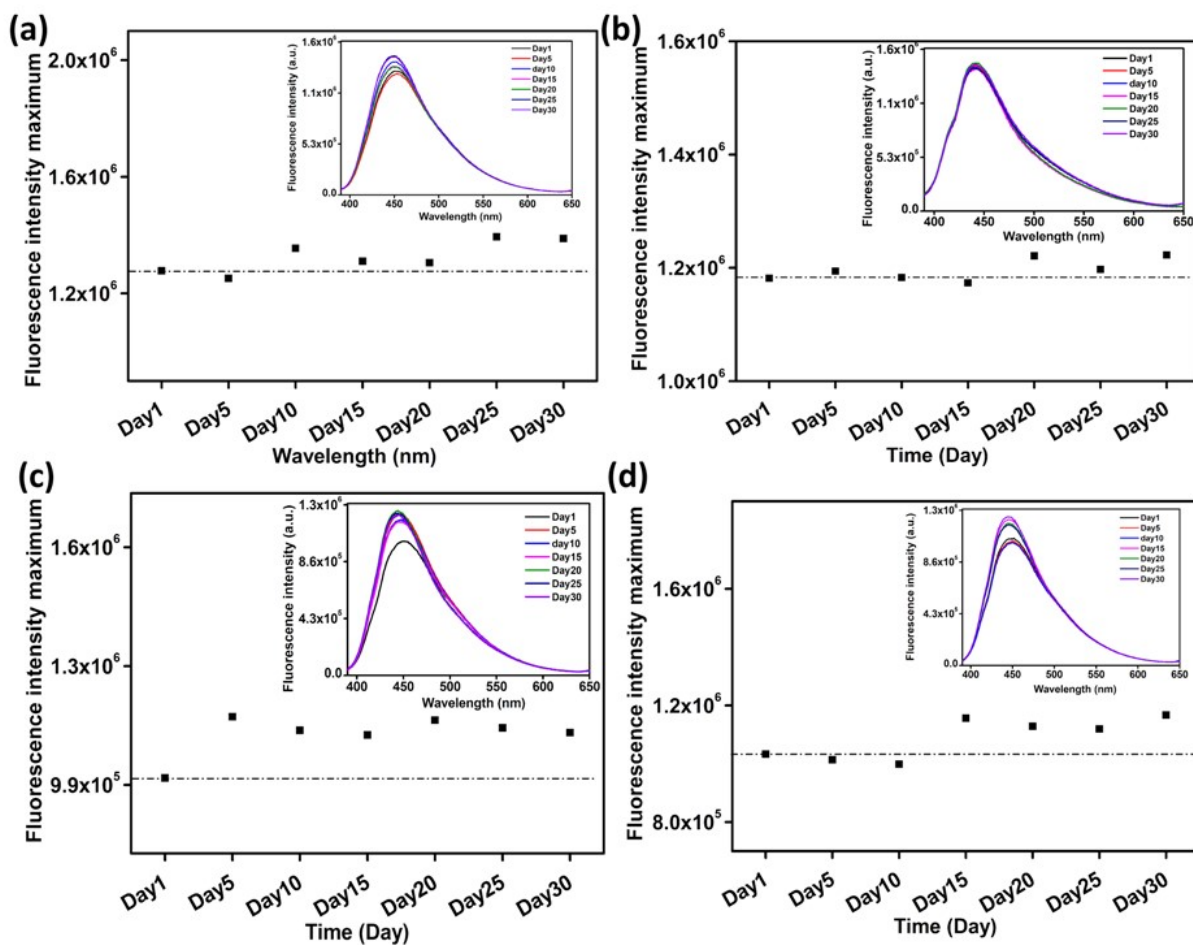


**Figure S3:** Variation of fluorescence intensity of synthesized ZnS-GT QDs as function of storage time in the presence of different metal ions. (a)  $K^+$ , (b)  $Na^+$ , (c)  $Ca^{2+}$  and (d)  $Co^{2+}$  in phaophate buffer of pH 8.0.

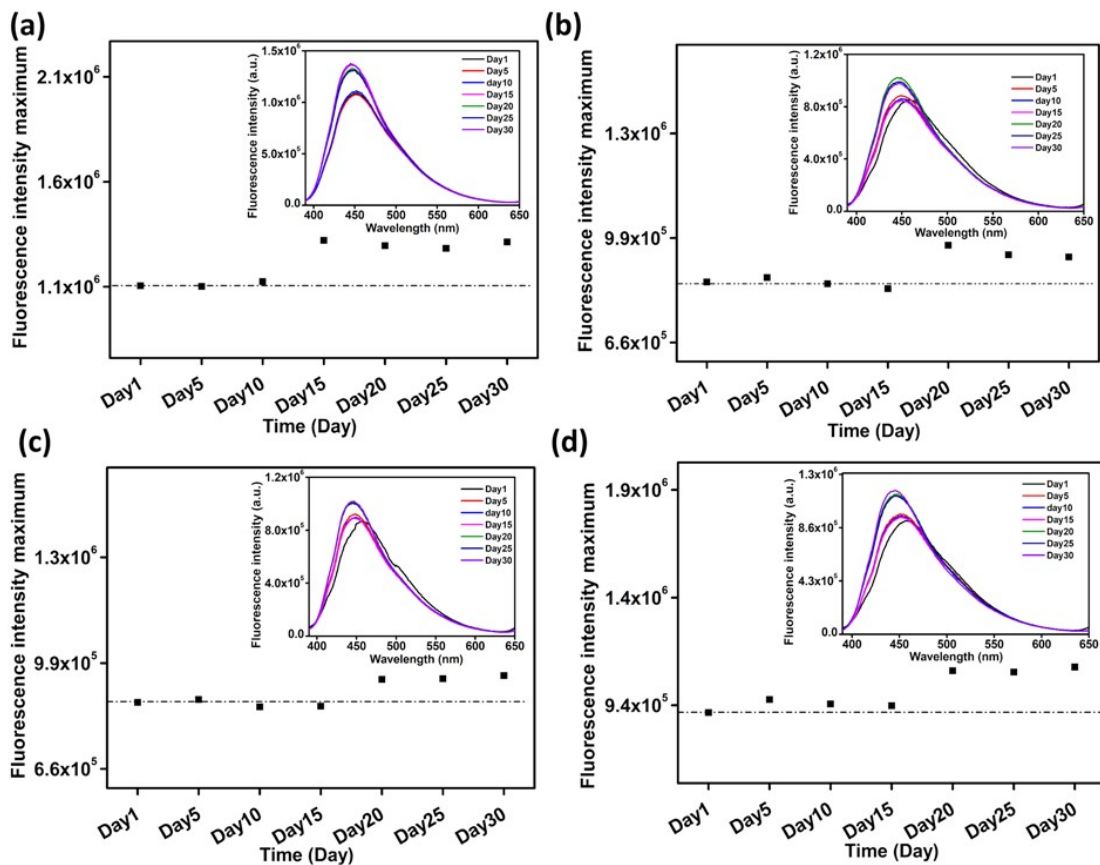


**Figure S4:** Variation of fluorescence intensity of synthesized ZnS-GT QDs as function of storage time in the presence of different metal ions. (a)  $\text{Cu}^{2+}$ , (b)  $\text{Ni}^{2+}$  (c)  $\text{Fe}^{3+}$  and (d)  $\text{Fe}^{2+}$  in phosphate buffer of pH 8.0.



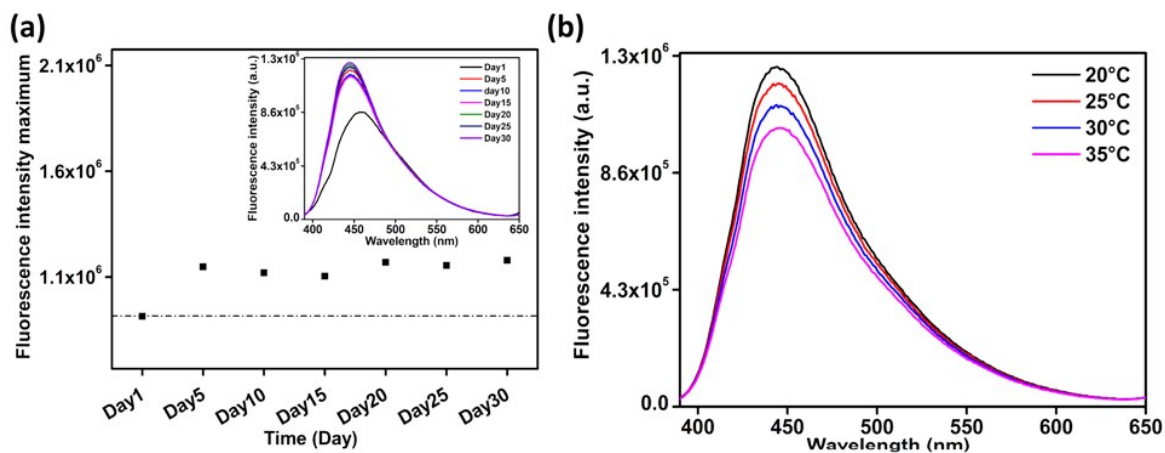


**Figure S5:** (a) Variation of fluorescence intensity of synthesized ZnS-GT QDs as function of storage time in the presence of  $\text{Mn}^{2+}$  ion and (b) effect of temperature on ZnS-GT QDs fluorescence intensity.

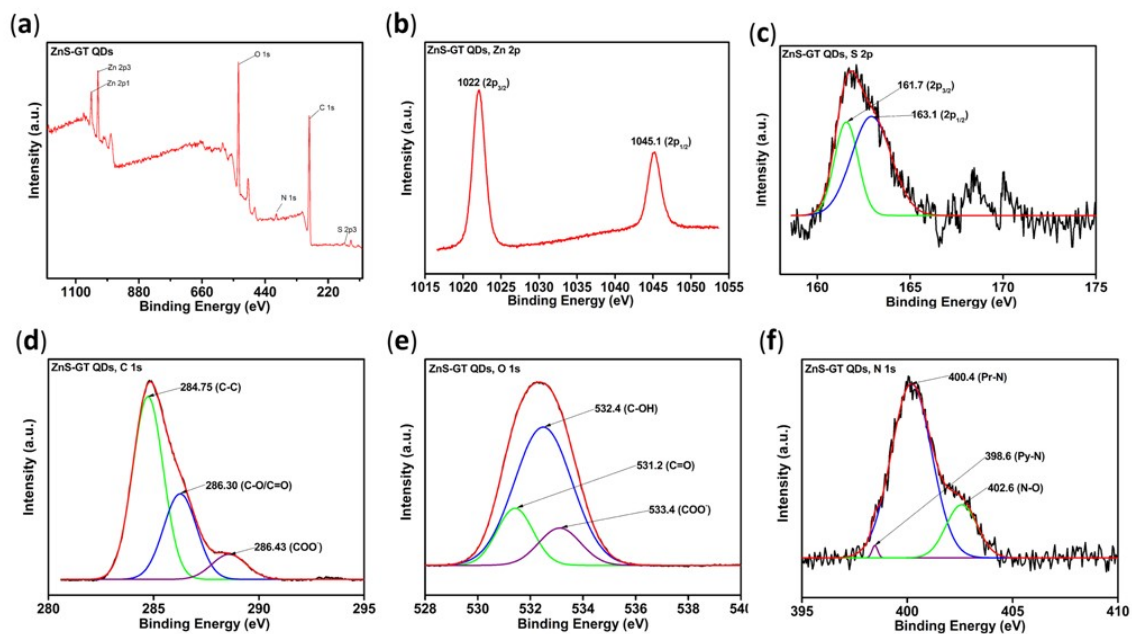


**Figure S6:** XPS spectra of synthesized ZnS-GT QDs. (a) survey spectrum, (b) Zn 2p, (c) S 2p, (d) C 1s, (e) O 1s and (f) N 1s spectra of ZnS-GT QDs.

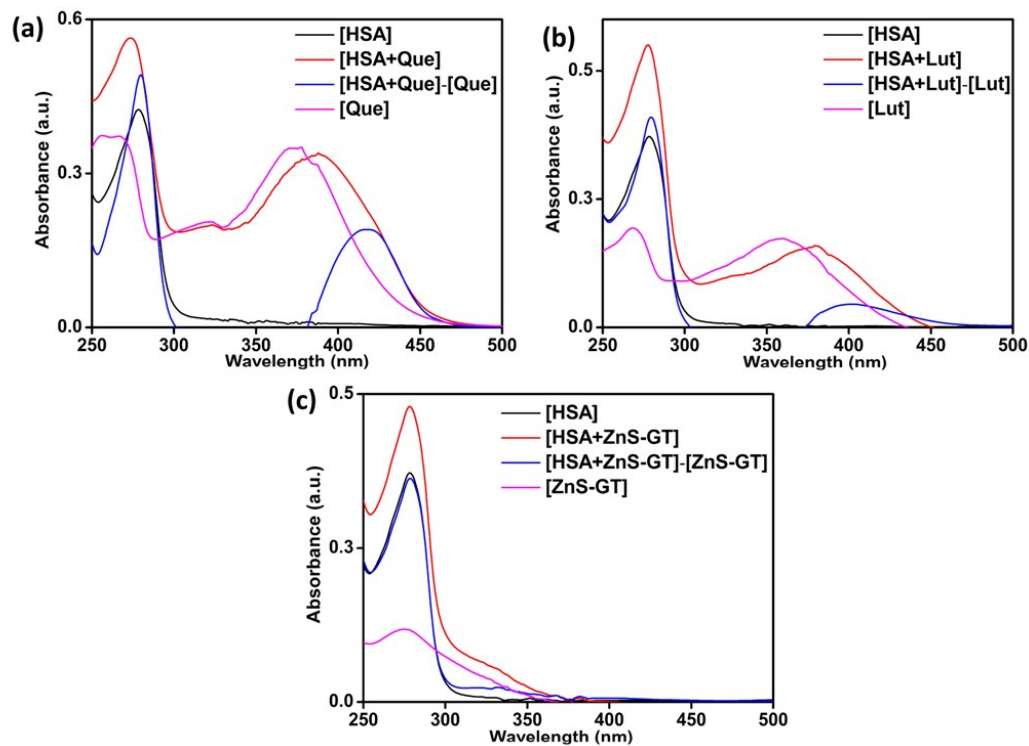


**Figure S7:** Absorption profile of 10  $\mu\text{M}$  HSA and their 1:1 complexes. (a) Que, (b) Lut and (c) ZnS-GT QDs in 20 mM phosphate buffer of pH 7.4.

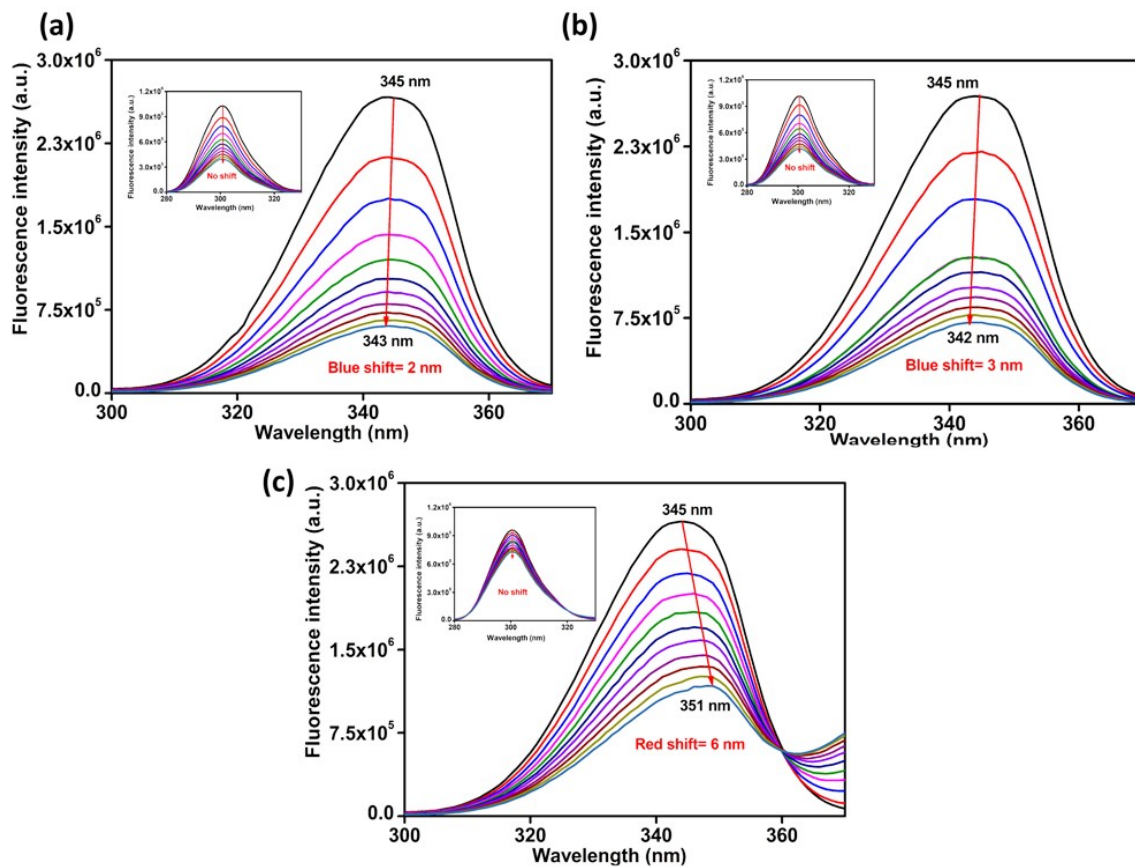


**Figure S8:** Synchronous fluorescence spectra of HSA (3  $\mu$ M) protein in the presence of ligands (0-9.97  $\mu$ M). (a) Quercetin (Que), (b) Luteolin (Lut) and (c) ZnS-GT QDs in 20 mM phosphate buffer of pH 7.4.

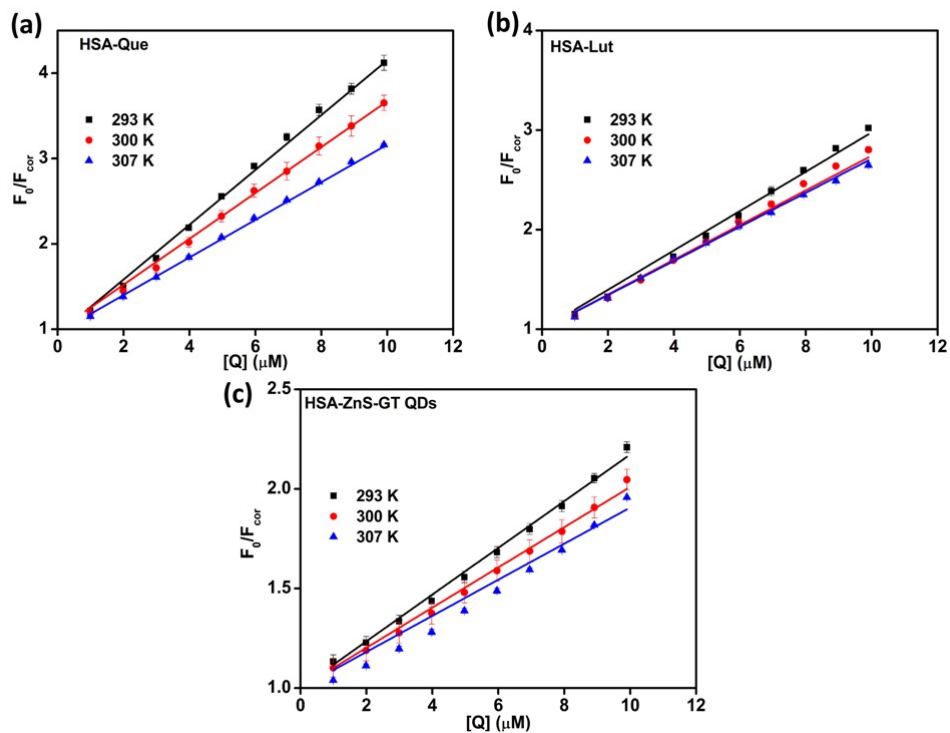


**Figure S9:** Stern-Volmer plot for the interaction of ligands (0-9.97  $\mu\text{M}$ ) with HSA (3  $\mu\text{M}$ ) at various temperatures. (a) HSA-Que, (b) HSA-Lut and (c) HSA-ZnS-GT QDs binding in 20 mM phosphate buffer of pH 7.4.

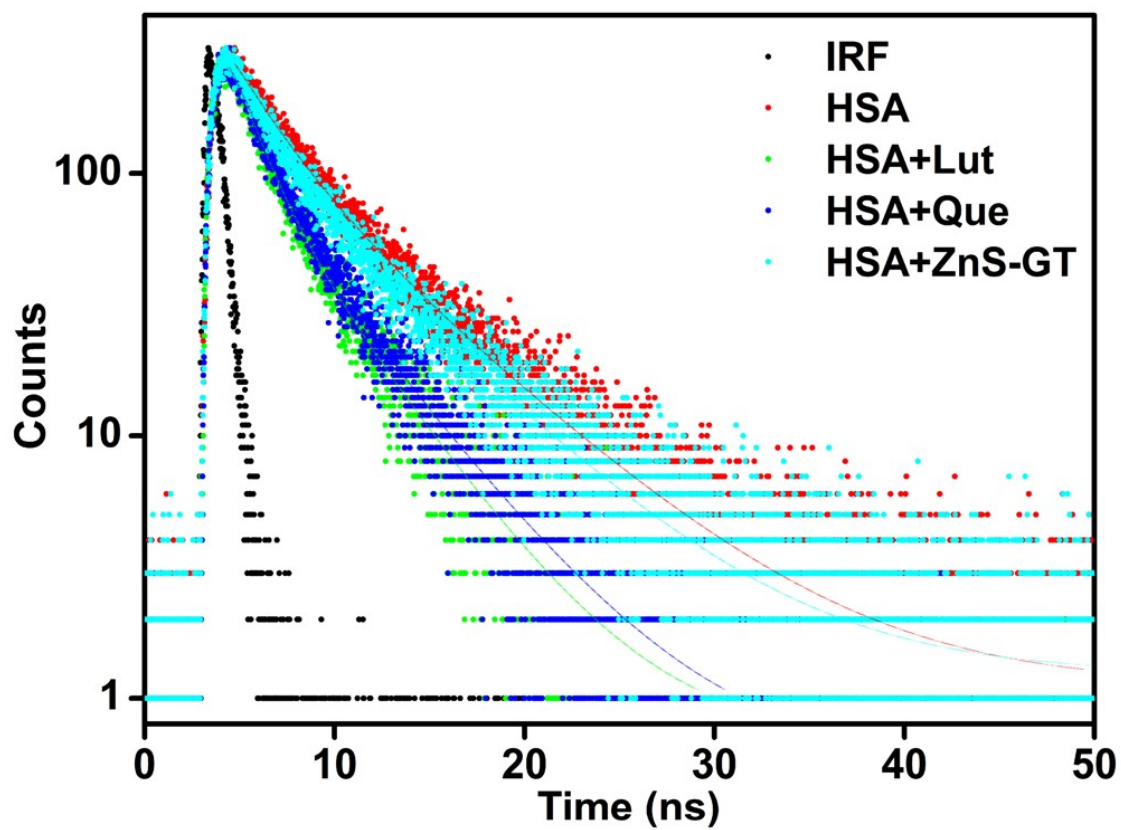


**Figure S10:** Lifetime decay profiles of HSA protein ( $\mu\text{M}$ ) and their complexes with Lut, Que and ZnS-GT QDs at a molar ratio 1:2.

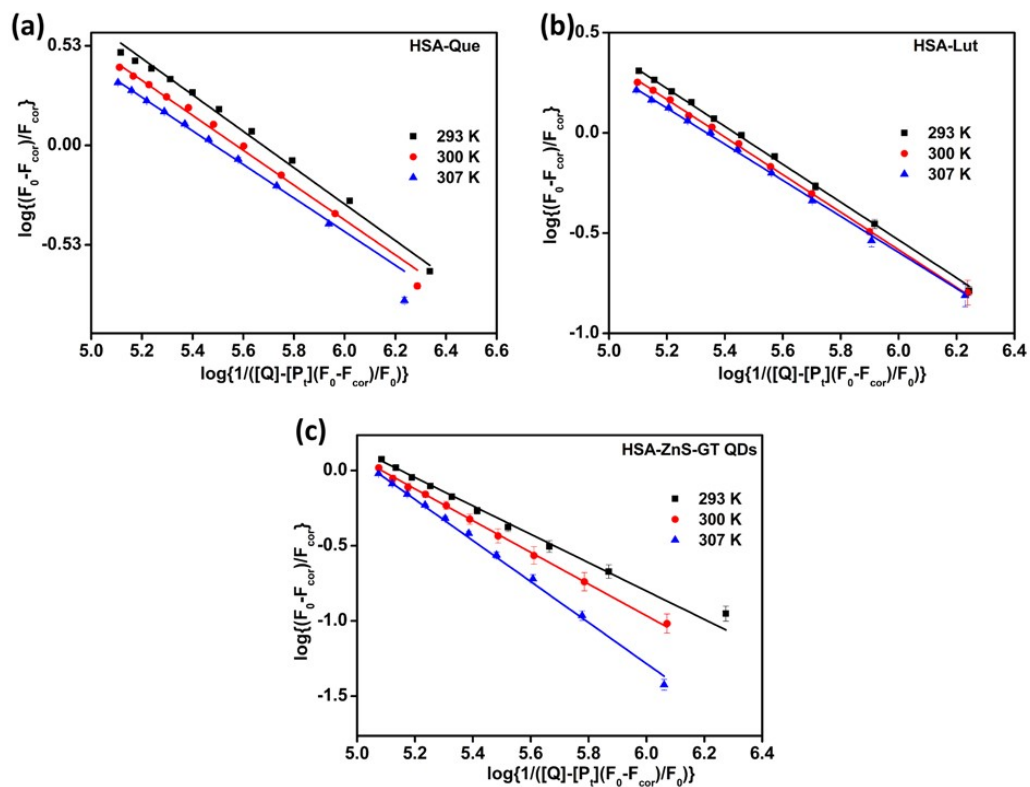


**Figure S11:** Double log plot for the interaction of ligands (0-9.97  $\mu\text{M}$ ) with HSA (3  $\mu\text{M}$ ) at different temperatures. (a) HSA-Que, (b) HSA-Lut and (c) HSA-ZnS-GT QDs binding in 20 mM phosphate buffer of pH 7.4.

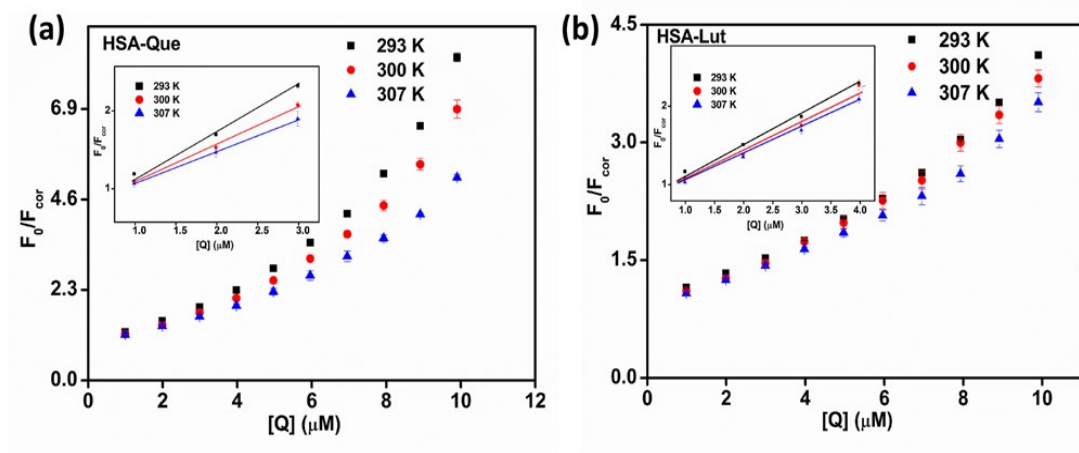


**Figure S12:** Stern-Volmer plot (a) HSA-Que and (b) HSA-Lut interactions in the presence of ZnS-GT QDs (9.97  $\mu\text{M}$ ) in 20 mM phosphate buffer of pH 7.4.  $[\text{Que}] = [\text{Lut}] = (0-9.97 \mu\text{M})$



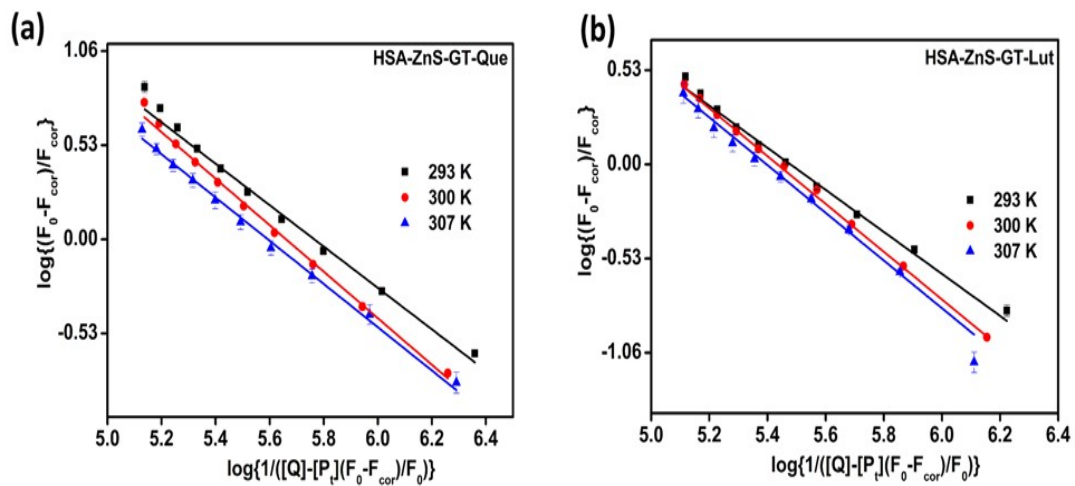


**Figure S13:** Double log plot (a) HSA-Que and (b) HSA-Lut interactions in the presence of ZnS-GT QDs (9.97  $\mu$ M) in 20 mM phosphate buffer of pH 7.4. [Que]=[Lut]= (0-9.97  $\mu$ M)

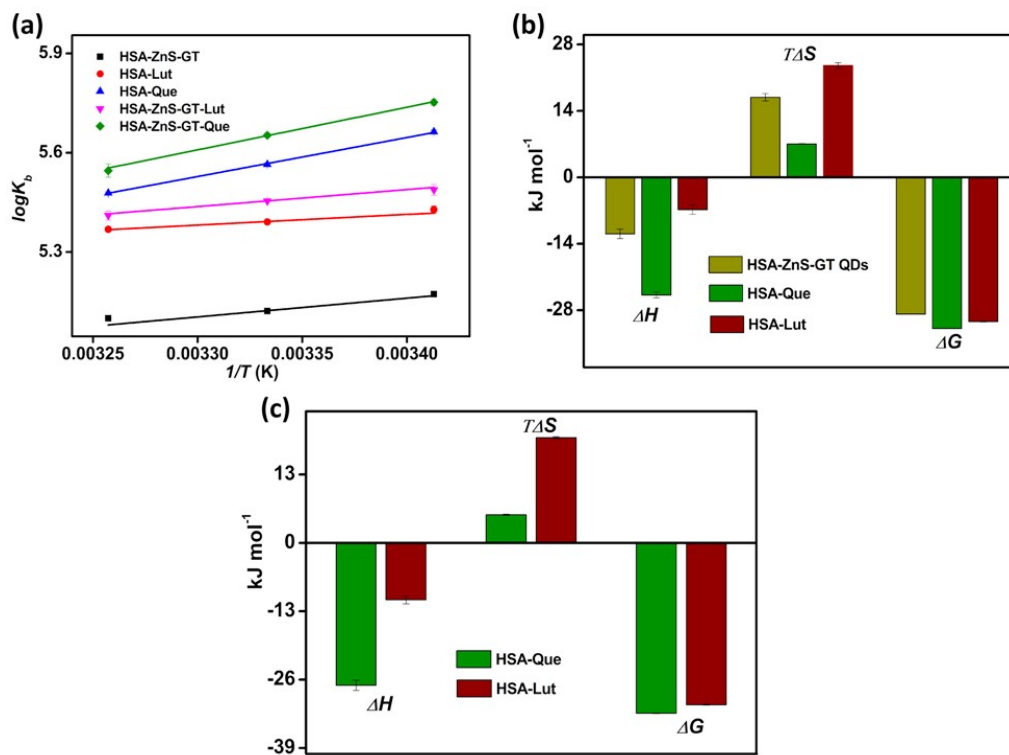


**Figure S14:** (a)  $\log K_b$  vs  $1/T$  Plot, (b) representation of thermodynamic parameters of ZnS-GT QDs, Que, and Lut with HSA and (c) thermodynamic parameters of HSA-Que and HSA-Lut interactions in the presence of ZnS-GT QDs.

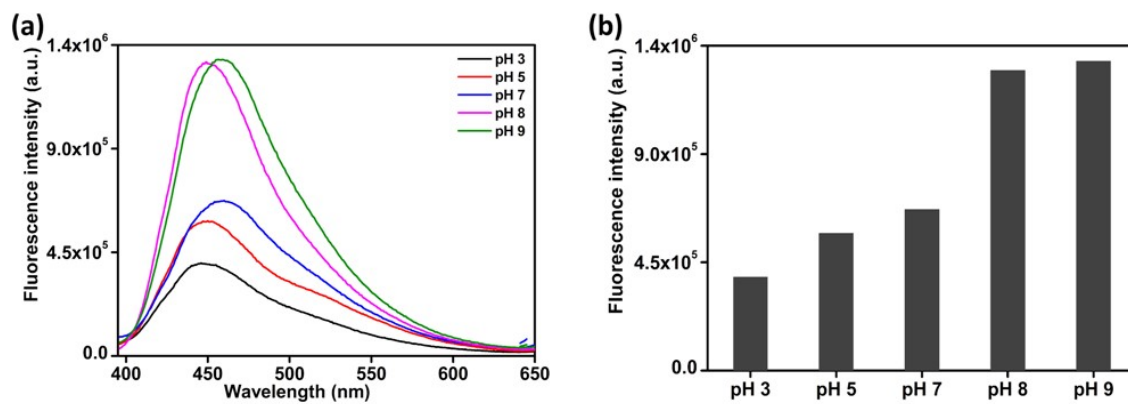


**Figure S15:** Effect pH (phosphate buffer) on the fluorescence intensity of ZnS-GT QDs.

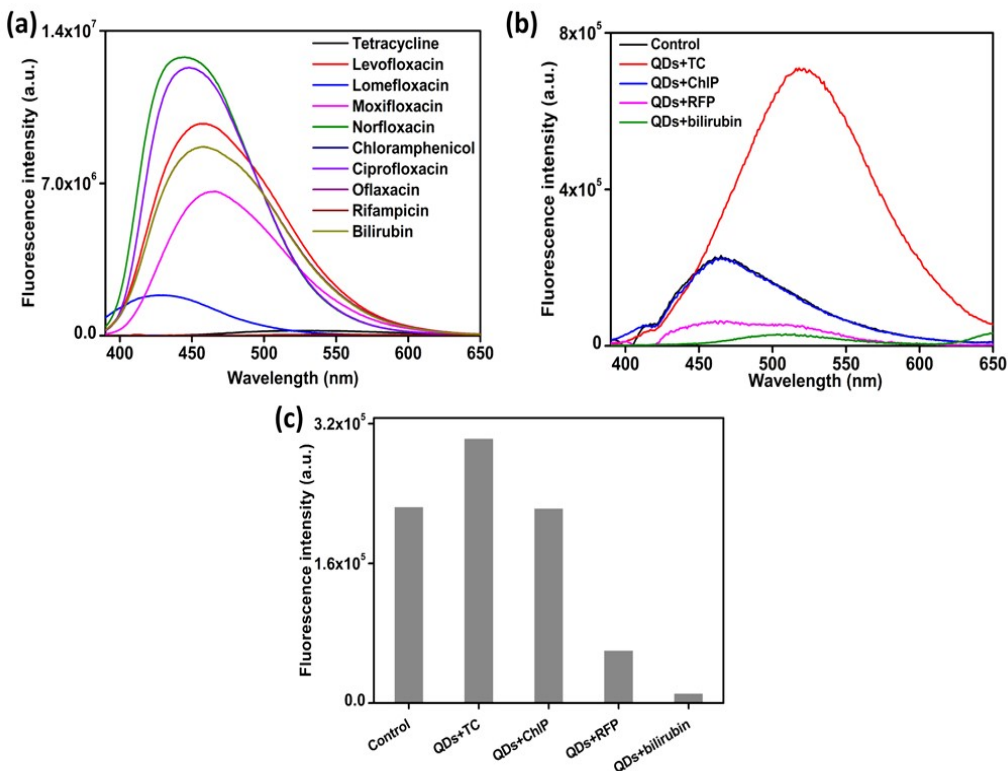


**Figure S16:** (a) Emission spectra of various antibiotics (30 μM), (b) fluorescence emission of ZnS-GT QDs (3 μM) in the absence (control) and presence of tetracycline (TC), chloramphenicol (ChlP), rifampicin (RFP), and bilirubin and (c) depicted the bar diagram. Concentration of all the antibiotics is 30 μM.

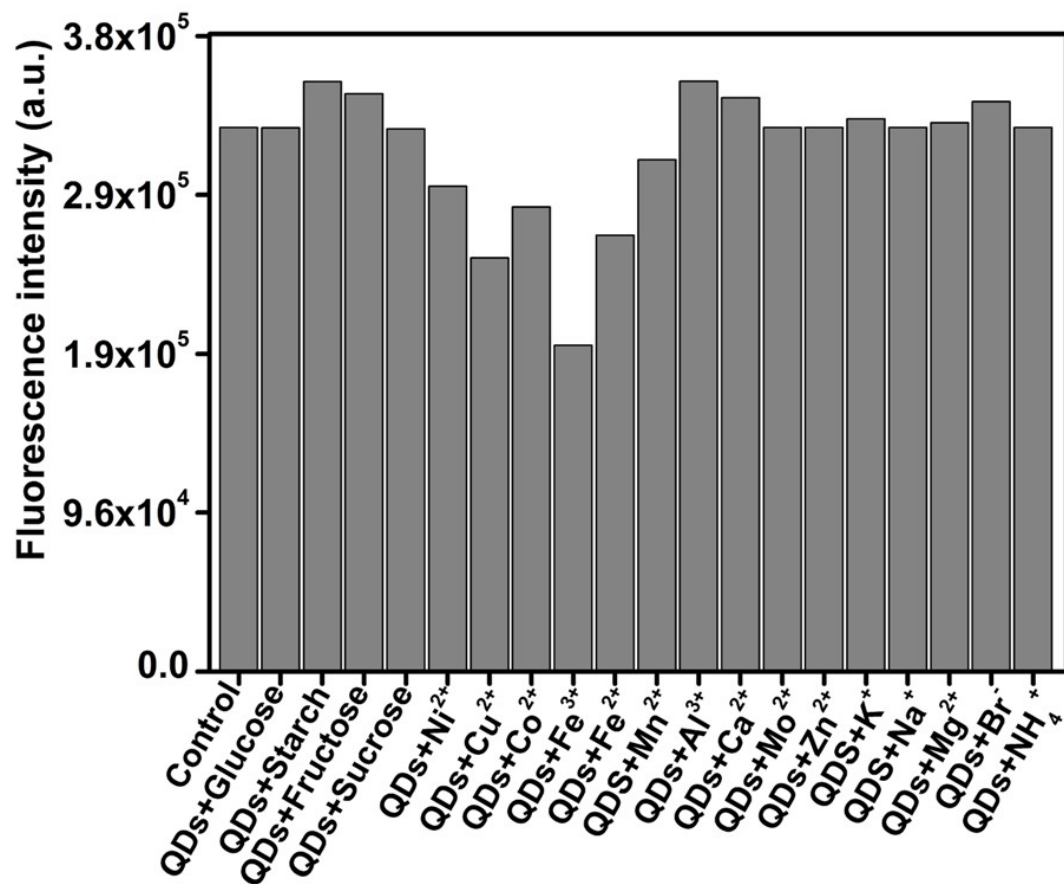


**Figure S17:** Effect of interfering agents on the fluorescence intensity of ZnS-GT QDs. [ZnS-GT QD] = 20  $\mu$ M, [Interfering agents] = 5  $\mu$ g/mL.

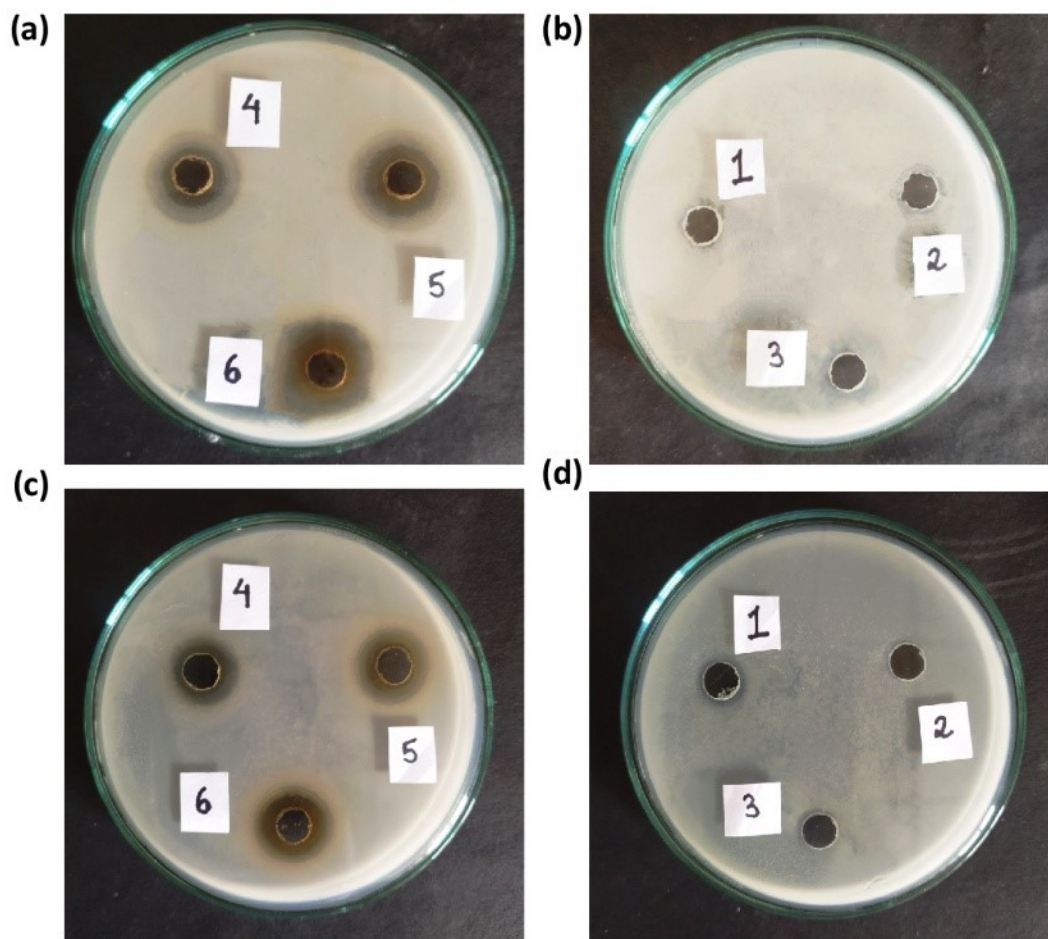


**Figure S18:** ZOI of ZnS-GT QDs against (a) *E. coli* and (c) *E. faecalis* {10 (4), 15(5), and 20 (6)  $\mu\text{g mL}^{-1}$ } and their respective control represented in (b), (d);  $\text{Zn}(\text{CH}_3\text{COO})_2$  (1), water (2) and GT extract (3).

**Table S1:** Observed FTIR peaks in bio-synthesized ZnS-GT QDs and neat green tea extract

SL No.	Reference peak	GT extract peak (cm <sup>-1</sup> )	ZnS-GT QDs peak (cm <sup>-1</sup> )	Shift of peak position (if any) (cm <sup>-1</sup> )
1	O-H stretching of aromatic alcohol	3352	3347	5
2	N-H vibrational frequency of amino acid (-NH <sub>3</sub> )	2973	-	
3	C-H (alkanes) stretching frequency	2926	2921	5
4	O-H stretching frequency (carboxylic acid)	2853	2850	3
5	C=O stretching of ester	1698	-	
6	C=O stretching of amide	1639	1602	37
7	N-H bending of amide	1456	1427	29
8	O-H bending in the plane	1374	1338	36
9	O-H aromatic vibration	1147	1141	6
10	C-O stretching of amine	1036	-	
11	Zn-S vibration	-	1058	
12	Zn-S vibration	-	618	

**Table S2:** The quenching parameters  $K_{SV}$  and  $K_q$  for the HSA-ligands interactions (ligands: quercetin: Que, luteolin: Lut and ZnS GT QDs)

	<b>Temp. (K)</b>	<b><math>K_{SV}</math> (<math>10^5 \text{ M}^{-1}</math>)</b>	<b><math>k_q</math> (<math>10^{13} \text{ M}^{-1}\text{s}^{-1}</math>)</b>
<b>HSA-Que</b>	293	3.153±0.054	6.306±0.108
	300	2.663±0.126	5.236±0.253
	307	2.173±0.012	4.346±0.025
<b>HSA-Lut</b>	293	1.983±0.038	3.966±0.077
	300	1.806±0.023	3.613±0.047
	307	1.686±0.024	3.373±0.049
<b>HSA-ZnS-GT</b>	293	1.166±0.037	2.333±0.075
	300	1.006±0.078	2.013±0.156
	307	0.856±0.020	0.171±0.004



**Table S3:** Molecular recognition and thermodynamic parameters for the HSA-Que, HSA-Lut and HSA-ZnS-GT QDs interactions at various temperatures.

	Temp.(K)	$K_b(10^5, \text{M}^{-1})$	$n$	$\Delta H (\text{kJ mol}^{-1})$	$\Delta S (\text{JK}^{-1} \text{mol}^{-1})$	$\Delta G (\text{kJ mol}^{-1})$
<b>HSA-Que</b>	293	4.781±0.068	0.945±0.021	-(24.811±0.605)	+(24.029±0.200)	-(31.862±0.033)
	300	3.726±0.040	0.962±0.018			-(32.002±0.027)
	307	2.975±0.008	0.999±0.021			-(32.191±0.020)
<b>HSA-Lut</b>	293	2.636±0.077	0.989±0.027	-(6.696±0.985)	+(80.383±1.980)	-(30.311±0.070)
	300	2.397±0.016	1.054±0.072			-(30.902±0.017)
	307	2.267±0.021	1.071±0.070			-(31.480±0.023)
<b>HSA-ZnS-GT</b>	293	1.380±0.092	0.885±0.115	-(11.929±1.009)	+(57.608±2.684)	-(28.835±0.016)
	300	1.212±0.032	1.177±0.098			-(29.200±0.006)
	307	1.138±0.024	1.326±0.076			-(29.740±0.034)

**Table S4:** The quenching parameters ( $K_{SV}$  and  $K_q$ ) HSA-Que and HSA-Lut interactions in the presence ZnS-GT QDs.

	<b>Temp. (K)</b>	<b><math>K_{SV}</math> (<math>10^5</math>, M<sup>-1</sup>)</b>	<b><math>k_q</math> (<math>10^{13}</math>, M<sup>-1</sup>s<sup>-1</sup>)</b>
HSA-ZnS-GT-Que	293	3.023±0.044	6.046±0.089
	300	2.680±0.180	5.360±0.361
	307	2.245±0.145	4.490±0.290
HSA-ZnS-GT-Lut	293	1.903±0.061	3.806±0.122
	300	1.675±0.005	3.350±0.001
	307	1.565±0.065	3.130±0.013

**Table S5:** Reported LOD value for the detection of bilirubin and RFP.

	Methods	Sensing Probe	Concentration range	LOD values	Reference
Bilirubin	DLS	HSA-Carboxyl QDs	0-150 nM	0.6 nM	<sup>8</sup>
	Electrochemical sensing	RGO-PSS	0-450 $\mu$ M	2.0 $\mu$ M	<sup>9</sup>
	Fluorometry	HSA-AU NCs	0-75 $\mu$ M	248 $\pm$ 12nM	<sup>10</sup>
	Calorimetric	HSA-AU NCs	-	200 $\pm$ 19 nM	<sup>10</sup>
	Fluorometry	CdS GT QDs	5-50 $\mu$ M	2.90 $\pm$ 0.05 ng/mL	<sup>11</sup>
	Fluorometry	ZnS-GT QDs	0-30 $\mu$ M	22.12 $\pm$ 0.25 ng/mL	Present work
RFP	Fluorometry	GSH-CdTe/ZnS QDs	4.05-36.45 $\mu$ M	0.06 $\mu$ M/L	<sup>12</sup>
	Fluorometry	BSA-Au NCs	0.5-823 $\mu$ g/mL	70 ng/mL	<sup>13</sup>
	Fluorometry	MPA-CdTe QDs	5-80 $\mu$ g/mL	1.5 $\mu$ g/mL	<sup>14</sup>
	Fluorometry	CdS GT QDs	5-50 $\mu$ M	141.010 $\pm$ 1.4 ng/mL	<sup>11</sup>
	Fluorometry	ZnS-GT QDs	0-30 $\mu$ M	122.37 $\pm$ 0.42 ng/mL	Present work

**Table S6:** Effect of interfering substances on ZnS-GT QDs fluorescence

Interfering agents	Conc. (µg/mL)	ZnS-GT QDs fluorescence intensity (%)	Interfering agents	Conc. (µg/mL)	ZnS-GT QDs fluorescence intensity (%)
<b>Glucose</b>	0.1	+0.1	$\text{Al}^{3+}$	0.1	+2.4
	1	+0.3		1	+4.9
	5	+1.3		5	+8.8
<b>Starch</b>	0.1	+0.3	$\text{Ca}^{2+}$	0.1	+0.4
	1	+1.1		1	+0.9
	5	+6.2		5	+5.5
<b>Fructose</b>	0.1	+0.8	$\text{Mo}^{2+}$	0.1	+0.7
	1	0.9		1	+2.0
	5	+5.1		5	+4.6
<b>Sucrose</b>	0.1	-0.1	$\text{Zn}^{2+}$	0.1	+0.9
	1	-0.4		1	+1.7
	5	-0.6		5	+3.8
$\text{Ni}^{2+}$	0.1	-0.4	$\text{K}^{+}$	0.1	+0.1
	1	-1.6		1	+0.7
	5	-8.3		5	+1.0
$\text{Cu}^{2+}$	0.1	-0.9	$\text{Na}^{+}$	0.1	+0.1
	1	-3.8		1	+0.3
	5	-19.7		5	+0.6
$\text{Co}^{2+}$	0.1	-1.3	$\text{Mg}^{2+}$	0.1	+0.6
	1	-4.6		1	+1.2
	5	-14.8		5	+2.9
$\text{Fe}^{3+}$	0.1	-4.3	$\text{Br}^{-}$	0.1	+1.6
	1	-11.5		1	+2.4
	5	-31.9		5	+4.7
$\text{Fe}^{2+}$	0.1	-3.1	$\text{NH}_4^{+}$	0.1	+0.9
	1	-8.4		1	+3.3
	5	-22.7		5	+5.1
$\text{Mn}^{2+}$	0.1	-0.7			
	1	-1.2			
	5	-4.4			

+ve sign: Enhanced fluorescence intensity

-ve sign: Quenching of fluorescence intensity

**Table S7:** Percentage cell viability of untreated (control) and ZnS-GT QDs treated HeLa cells.

	<b>Concentration (<math>\mu\text{g/mL}</math>)</b>	<b>Absorbance (570 nm)</b>	<b>% cell viability</b>
Untreated HeLa Cell	-	1.244 $\pm$ 0.009	100
ZnS-GT QDs treated	10	0.750 $\pm$ 0.007	59.8
HeLa Cell	25	0.307 $\pm$ 0.001	24.4
GT extract treated HeLa cell	25	1.201 $\pm$ 0.014	95.8

## References

- 1 D. F. Eaton, *J. Photochem. Photobiol. B Biol.*, 1988, **2**, 523–531.
- 2 W. Zhou, D. T. Schwartz and F. Baneyx, *J. Am. Chem. Soc.*, 2010, **132**, 4731–4738.
- 3 N. H. Abdullah, Z. Zainal, S. Silong, M. I. M. Tahir, K. B. Tan and S. K. Chang, *Mater. Chem. Phys.*, 2016, **173**, 33–41.
- 4 S. K. Mani, S. Manickam, V. Muthusamy and R. Thangaraj, *J. Nanostructures*, 2018, **8**, 107–118.
- 5 K. Abha, J. Nebu, J. S. Anjali Devi, R. S. Aparna, R. R. Anjana, A. O. Aswathy and S. George, *Sensors Actuators, B Chem.*, 2019, **282**, 300–308.
- 6 J. B. F. LLOYD, *Nat. Phys. Sci.*, 1971, **231**, 64–65.
- 7 J. N. Miller, *Proc. Anal. Div. Chem. Soc.*, 1979, **16**, 203–208.
- 8 W. Zhao, C. Zong, T. Lei, W. Tian, M. Sun, X. Liu, Q. Zhang and H. Gai, *Sensors Actuators, B Chem.*, 2018, **275**, 95–100.
- 9 T. Balamurugan and S. Berchmans, *RSC Adv.*, 2015, **5**, 50470–50477.
- 10 M. Santhosh, S. R. Chinnadayala, A. Kakoti and P. Goswami, *Biosens. Bioelectron.*, 2014, **59**, 370–376.
- 11 M. Haque, S. Lyndem and A. Singha Roy, *Luminescence*, 2022, **37**, 837–853.
- 12 Z. Hooshyar and G. R. Bardajee, *Spectrochim. Acta - Part A Mol. Biomol. Spectrosc.*, 2017, **173**, 144–150.
- 13 K. Chatterjee, W. C. Kuo, A. Chen and P. Chen, *J. Nanobiotechnology*, 2015, **13**, 1–9.
- 14 J. Jimenez-López, L. Molina-García, S. S. M. Rodrigues, J. L. M. Santos, P. Ortega-Barrales and A. Ruiz-Medina, *J. Lumin.*, 2016, **175**, 158–164.